ANALYZES OF VERY HIGH-Q QUARTZ CRYSTAL AIMED TO HIGH QUALITY 5 MHZ RESONATORS ACHIEVEMENT

J. Imbaud[(1)], J.J. Boy[(1)], J.P. Romand[(1)], J. Frayret[(2)], D. Picchedda[(3)], G. Cibiel[(4)] and F. Sthal[(1)]

[(1)] Time and Frequency Dept., FEMTO-ST, CNRS, ENSMM, UFC, UTBM, Besançon, France
[(2)] LCABIE, IPREM, UMR CNRS 5254, Université de Pau et des Pays de l'Adour, Pau, France
[(3)] GEMMA Quartz & Crystal, Annecy, France
[(4)] Microwave and Time-Frequency Department, CNES, Toulouse, France
Joel.Imbaud@ens2m.fr

Abstract

This article reports analyzes on a specific quartz crystal block supplied for a specific program on 1/f noise of quartz crystal resonator. This kind of synthetic crystal is usually used to growth new generation of quartz crystal blocks. Description of the blanks realization is presented. Inclusions detection by optical methods are studied. FTIR Spectrometry for mapping alpha values and ICP-MS measurements to qualify amount chemical impurities of the crystal are also given. The results about crystal quality are discussed.

INTRODUCTION

In the 90's, output frequency of a quartz crystal oscillator has reached stabilities in the upper 10^{-14} (flicker floor of the Allan deviation $\sigma_y(\tau)$, which occurs at τ = 1..10 s). As a matter of fact, the highest stability was obtained with bulk acoustic wave quartz crystal resonators at 5 and 10 MHz. So, in the last ten years, the research for higher stabilities reaches a standstill, while space applications are more and more demanding.
Since 2006, FEMTO-ST Institute has started a research program on the origin of noise in 5 and 10 MHz quartz crystal resonators, managed by the French Centre National d'Etudes Spatiales (CNES) in which the main European manufacturers of high-stability resonators and oscillators participate. Furthermore, improvements of measurement bench of resonator noise are now well accomplished [1-4]. Fig. 1 shows the experimental set-up used to measure the resonator noise. It's a carrier suppression bench with a flicker floor in term of Allan deviation of about $8 \cdot 10^{-15}$. Components are optimized at 5 MHz and the frequency mixer is particularly chosen attentively. Its driving power is adapted according to the output power of the synthesizer and its phase noise characteristics.

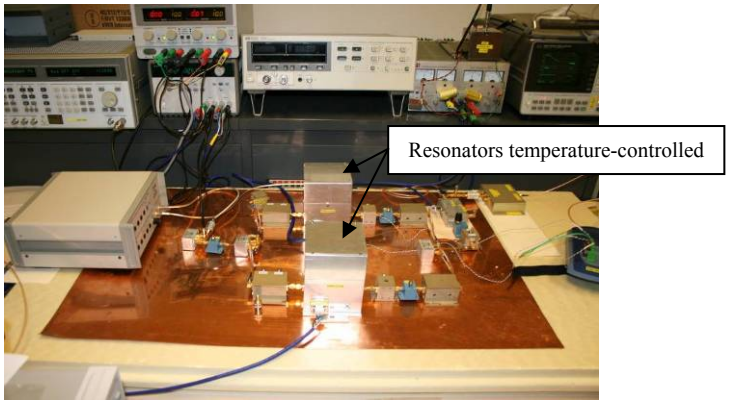

Fig. 1. Resonator noise measurement set-up.

Consequently, a new step of our study has now started. It consists on the realization of 5 MHz resonators with different manufacturing procedures in order to correlate the resonator noise with its fabrication parameters.
In this paper, the chosen resonator design parameters are described and discussed. This article reports also the first analyzes on a specific quartz crystal block supplied for this study. The quartz crystal study is well known and defined in the literature [5]. This kind of synthetic crystal is usually used to realize seeds to growth a new generation of quartz crystal blocks. Description of the blanks realization is presented. Inclusions detection by optical methods are studied. FTIR Spectrometry and ICP-MS measurements for mapping alpha values and amount chemical impurities of the crystal are given. The results about crystal quality are discussed.

CRYSTAL BLOCK AND RESONATOR SPECIFICATIONS

1/ Crystal block and first-cutting

The objective is to know precisely the position of the finished resonator into the quartz block. The C2 crystal block is presented in Fig. 2. This crystal block is obtained from a seed cut in a previous synthetic crystal which was grown using a natural seed. Its dimensions are approximately 220 mm along the Y-axis, 36 mm along the Z-axis and 110 mm along the X-axis. Two Y-cut slices have been cut before and after an oriented block used to achieve ten quartz bars (see red marks in Fig. 2). The Y-cut slices will be used to make X-ray topographies for dislocations evaluation.

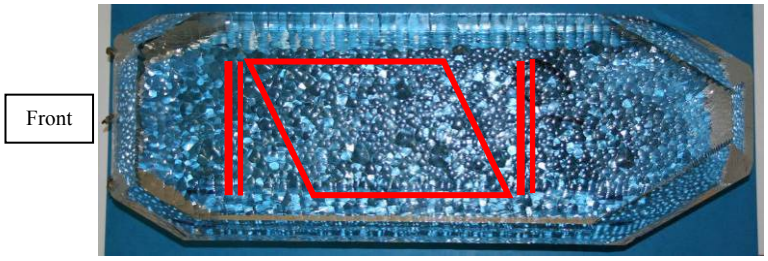

Fig. 2. C2 crystal block.

The crystal bars are cutting in order to get the double rotated SC-cut. Ten quartz bars pre-oriented on the φ angle (about 22° or 8° in respect with the vertical X-axis) have been achieved as seen in Fig. 3. The length of the bars is about 70 mm.

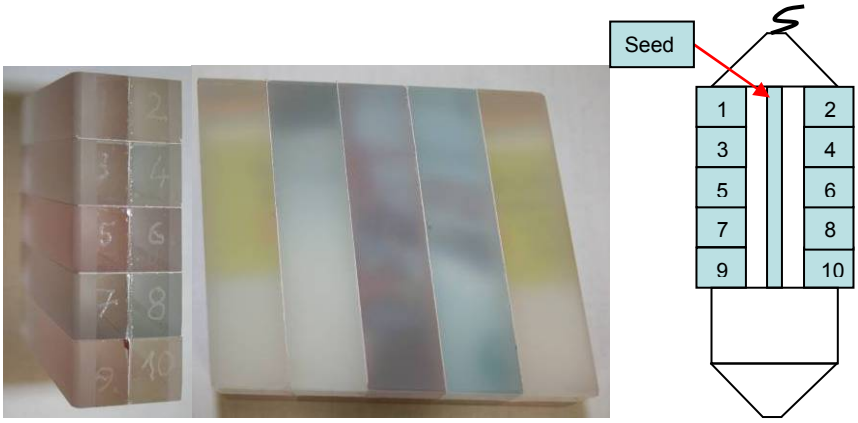

Fig. 3. Ten quartz crystal bars and their positions in the crystal.

2/ Final resonator specifications

The resonator specifications have been tested in a commercial crystal. The prototype of the resonator is a typical 5 MHz SC-cut resonator. The diameter of the resonator is 14 mm for a thickness of 1.09 mm. A plano-convex shape allows the energy trapping for the 3rd overtone of the slowest thickness shear mode (C-mode). A radius of curvature of 130 mm has been chosen to optimize this energy trapping according to the Tiersten-Stevens model [6]. Theoretically the ratio of the vibration amplitude from the center of the resonator to its edge is higher than 10^6. Electrodes diameter is 8 mm. The mode shape pattern obtained on a X-rays topography is presented in Fig. 4. It shows the optimized energy trapping of the C- mode vibration (300). The temperature turn over point of the resonator is chosen between 80 °C and 85 °C by adjusting the cut angles φ and θ.
The mean motional parameters and the unloaded quality factor are reported in the Table 1.

Table 1. Motional parameters and Q-factor of the prototype resonator.

	Expected values	Mean value on the 7 prototypes
Q-factor	$2.5 \cdot 10^6$	$2.4 \cdot 10^6$
R_x (Ω)	68	70
C_0 (pF)	5	5

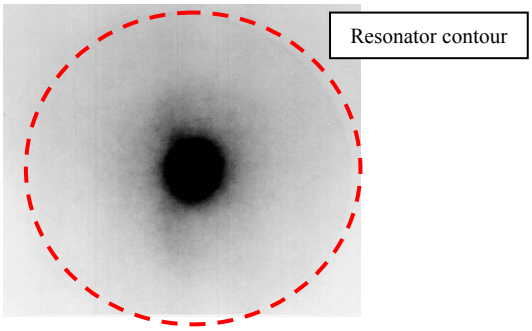

Fig. 4. X-ray topography of the resonator on its (300) vibration mode.

C2 CRYSTAL ANALYZES

1/ Infrared measurements

The infrared measurements are achieved with a FTIR spectrometer (Nicolet Magna 750). With IR transmission measurements at room temperature, the α parameter can be computed at 3500 cm^{-1}. It is defined according to the IEC758 standard. α expression is given by the following equation [7], where d is the thickness of the sample (generally chosen perpendicular to the Y-axis) expressed in cm:

$$\alpha_n = \frac{1}{d} Log \frac{T_{3800}}{T_n} \tag{1}$$

and T is the transmission in percent.

The "Time drive" concerns the measurement of the IR absorption rate along the quartz bar. The diameter of the IR beam is about 8 mm. Measurements are performed every 8 mm along the 70 mm of the bar. The thickness of the sample is equal to 14 mm. The Z-faces of all the 10 bars have been polished with 5 µm abrasive grains. As an example, Fig. 5 presents the α parameter for the quartz bar number 10.

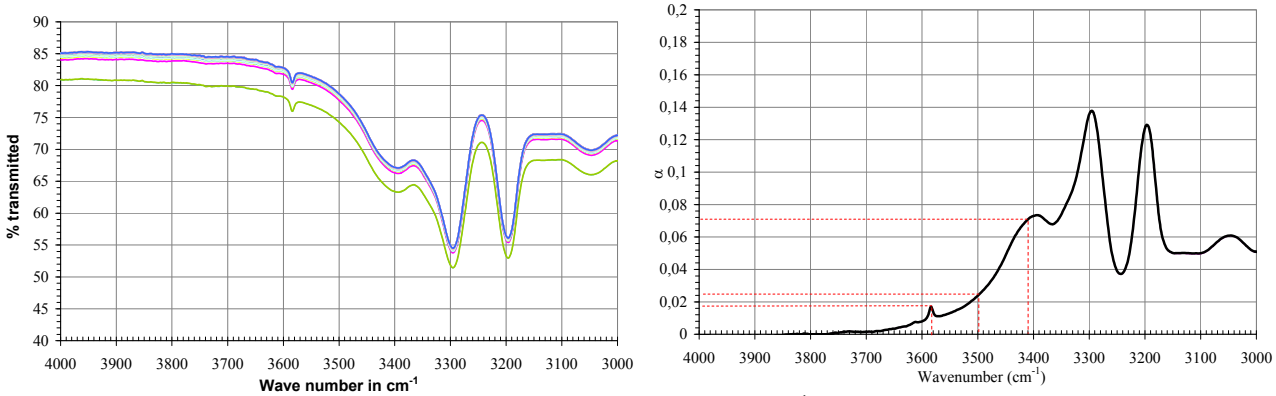

Fig. 5. Value of the IR transmission versus wavelength expressed in cm^{-1} (left) and α parameters (at 3410, 3500 and 3580 cm^{-1}) versus inverted wavelength of the 10th bar (right).

The α_{3410}, α_{3500} and α_{3585} are around 0.07, 0.023 and 0.016, respectively. These values correspond to high quality quartz crystal. The variation according to the different bars of the α_{3500} parameter is given in Fig. 6. The α_{3500} value is taken in the middle of each bar.

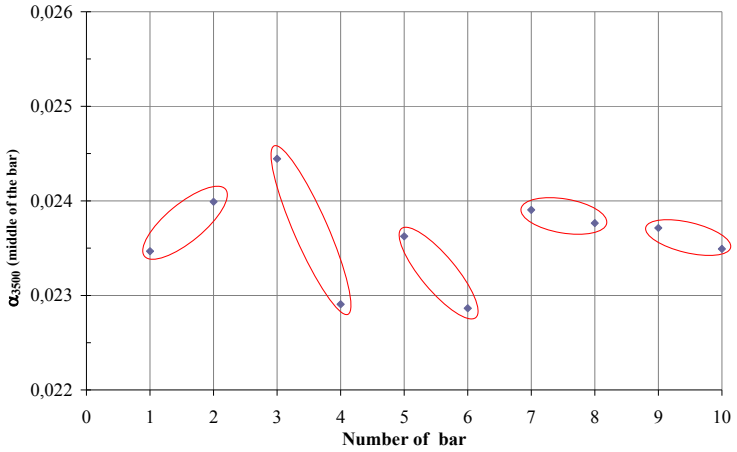

Fig. 6. Variations of α_{3500} localized in the middle of each quartz bar.

The values of α_{3500} remain close to 0.023 and fluctuations correspond to the spectrometer resolution. A mean value of $\alpha_{3500} = 0.0236\ cm^{-1}$ +/- $5 \cdot 10^{-4}$ has been computed. Alpha values are very homogeneous and there is no evident variation along the vertical axis of the pressure cell. The expected quality factor computed from an empirical relationship [8] gives a Q-value of about $2.8 \cdot 10^{6}$ for a reson ator working at 5 MHz.

2/ Defect detections

Experimental set-up is used in order to observe internal defects in quartz bar. Quartz bars are pre-oriented in φ direction in order to get the SC-cut plates. The optical Z-axis is used to propagate the HeNe beam. Fig. 7 shows the experimental installation. Transmission oil is used to attenuate the surface defects like scratches.

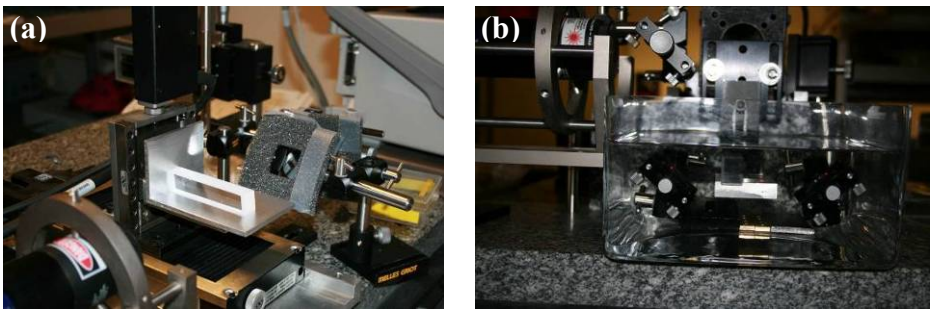

Fig. 7. a) HeNe transmission set-up in air, b) HeNe transmission set-up in oil.

The surface of the quartz bar scanned by the laser beam is shown in Fig. 8.

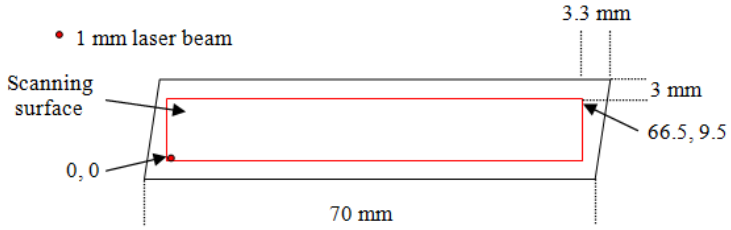

Fig. 8. HeNe scanned surface of the quartz bar.

Fig. 9 compares the optical signal transmission in air and in oil for one bar of the crystal. In air, interferences due to the parallelism face defect are clearly visible. In oil, the surface scratches are attenuated but predominant. Interpretation of the image remains difficult to detect internal defects because of the thickness integration.

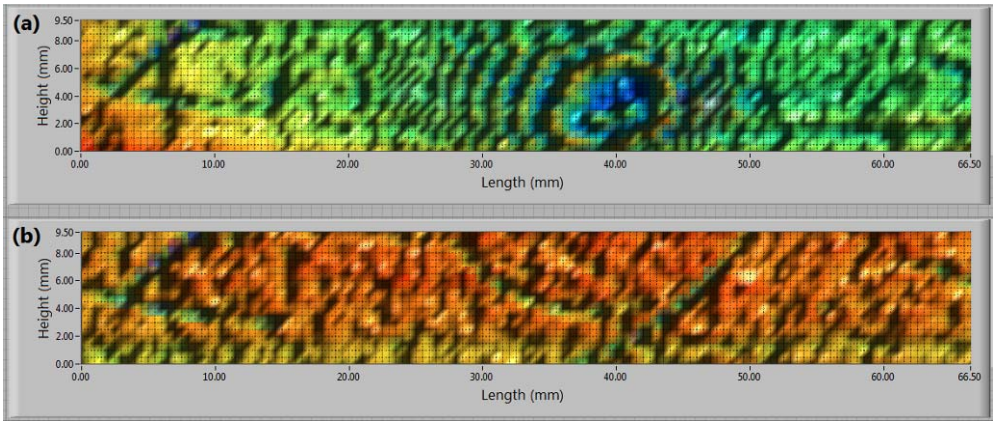

Fig. 9. In arbitrary unit, HeNe transmission signal through a quartz bar. a) quartz bar in air, b) quartz bar in oil.

In Fig. 10, a plate laser beam lights the crystal bar near the surface. Scratches are clearly visible in Fig. 10a. Fig. 10b shows the superposition of the HeNe scanning results on the optical picture. Fig 10c shows the 1 mm subsurface defects of the crystal bar. It seems that the number of inclusions is higher close to the seed than on the external surface. These defects can explain the contrast of the HeNe scanning results.

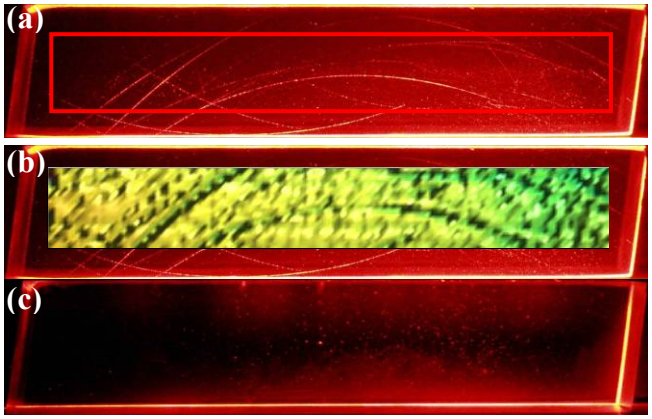

Fig. 10. Comparison between optical picture and the HeNe scanning, (a) Z surface of a crystal bar, (b) HeNe scanning superposed to optical picture, (c) 1 mm subsurface defects.

The IEC 49 standard defines the inclusion density by cm^3. This standard takes into account several sizes of inclusions. In the best grade (Ia), in which the C2 crystal is concerned, there are 10-30 µm, 30-70µm, 70-100 µm and above 100 µm sizes and the number of inclusions must be equal or lower to 3, 2, 1 and 1, respectively.
Fig. 11 shows the block lights with a white light beam. The big inclusions are clearly visible. The number of inclusions above 10 µm corresponds to the Grade Ia standard.

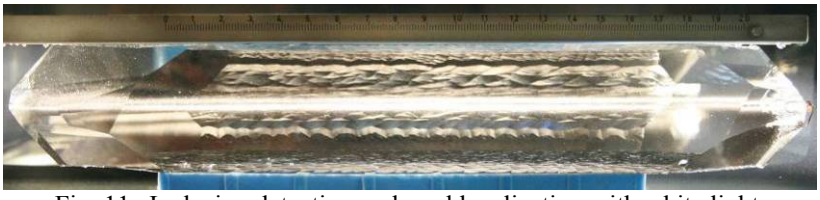

Fig. 11. Inclusion detection and seed localization with white light.

Another optical method using monochromatic laser beam was used to detect smaller inclusions. Fig. 12 shows the experimental set-up. A cylinder lens was used to obtain a linear (or planar) beam. The width of the beam is around 1 mm. Two HeNe lasers have been used, a red one at 632.8 nm with an output power of 35 mW and a green one at 543.5 nm with an output power of 5 mW. The lasers beams were moved to light the bar every mm along its X-axis. When the laser illuminates an inclusion, the light is scattered then an optical photo (with a camera) was taken every mm to locate all the inclusions in the crystal.

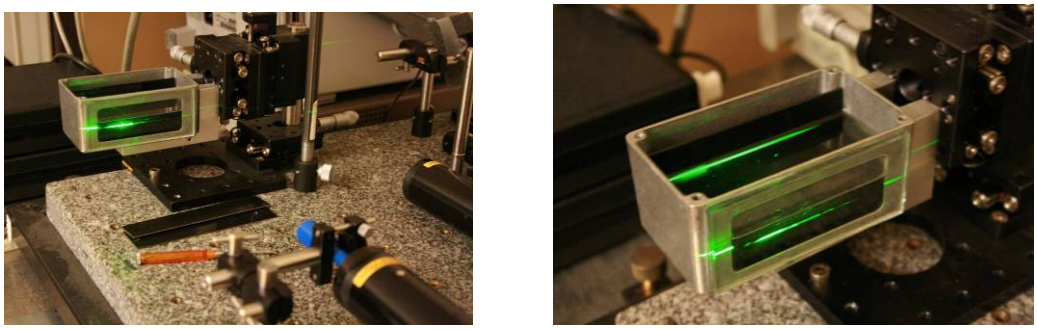

Fig. 12. Experimental set-up for detection of small size inclusions.

With this experiment, the optical view of the surface scratches indicates that the image resolution is below 10 µm. Defects with a diameter smaller than 5 µm are clearly visible in Fig. 13.

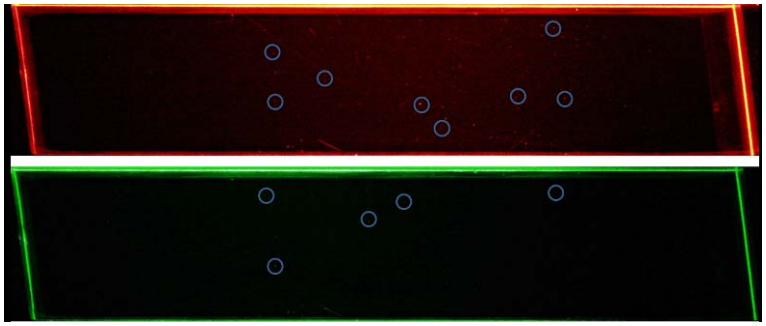

Fig. 13. Internal defects detected by the red and green HeNe laser scattering.

Table 2 shows a counting of these small defects in each crystal bar. The height of the bar corresponding to the X-face is around 14 mm. The picture taken near the side of the quartz seed can perturb the counting of the inclusions. Thus, the counting is made preferably in the middle of the bar height.

Table 2. Number of counted inclusions smaller than 1 µm in quartz bars.

Height (mm)	B1	B2	B3	B4	B5	B6	B7	B8	B9	B10
4	1	2	tm	tm	tm	tm	tm	7	tm	tm
5	4	4	tm	9	9	tm	tm	8	tm	8
6	4	9	14	13	13	tm	tm	2	12	6
7	1	0	16	3	3	21	12	2	9	8
8	1	5	14	8	8	6	7	1	9	1
9	0	4	11	0	0	4	4	0	2	0
10	0	1	5	4	4	9	1	2	1	0

tm : too many > 21

Typically, the number of inclusions is lower than 10 in the middle of each bar with a size lower than 1 µm. All the inclusions are now well located in the quartz bars.

3/ ICP-MS measurements

Chemical impurities of the C2 block have been measured by an inductively coupled plasma mass spectrometry technique (ICP-MS method). Analysis was performed with an ICPMS 7500ce from Agilent technologies (Tokyo, Japan). A certified reference material, the NIST 612 (National Institute of Standards and Technology, USA), was chosen to validate optimized working conditions, due to its low concentrations in some analyzed elements. About 3 grams of quartz samples were used for analysis. The preparation procedure was composed of three steps: cleaning, digestion and analysis. Table 3 presents the results of two samples from the triangular crystal parts before and after the bar block (see Fig. 2). The impurities rates are very low and seem homogeneous along the C2 crystal block. The Li concentration is similar in both samples. The concentrations of Al, Na, Li and K, lower than 0.1 ppm, correspond to a very high quality of the crystal even though the Ca concentration varies between 0.2 to 0.5 ppm. The Fe concentration

(lower than 1 ppm) seems to be more important at the front of the block and should ask more investigations to confirm this difference.

Table 3. Chemical impurities measured in the C2 block.

(in ppmw)	Front block	End block
Li	0.09 ± 0.03	0.1 ± 0.02
Na	< 0.07	< 0.05
Mg	< 0.0004	< 0.0003
Al	< 0.03	< 0.02
K	< 0.06	0.058 ± 0.001
Ca	0.22 ± 0.02	0.45 ± 0.03
Fe	0.98 ± 0.02	< 0.0001

CONCLUSION

This is the first time that a C2 quartz crystal will be used to manufacture high quality resonators. The crystal has been characterized by IR spectrometry and the α values are very homogeneous in the entire crystal, $\alpha_{3500} < 0.0236$ cm^{-1}. All the inclusions have been reported and are now well located in each crystal bar. Unfortunately the HeNe transmission did not permitted to conclude about internal defects other than inclusions. Chemical Impurities have been measured and confirm the very high quality of the crystal. The first step of the study concerning the crystal analyses is done and need to be cross with the future noise measurement.

REFERENCES

[1] F. Sthal, X. Vacheret, P. Salzenstein, S. Galliou, E. Rubiola, G. Cibiel, *"Advanced bridge instrument for the measurement of the phase noise and of the short-term frequency stability of ultra-stable quartz resonators"*, Proc. Joint Meeting IEEE Ann. Freq. Cont. Symp. and European Frequency and Time Forum, Genova, Switzerland, 29 May-1 June, pp. 254-260, (2007).

[2] S. Galliou, F. Sthal, X. Vacheret, R. Brendel, P. Salzenstein, E. Rubiola, G. Cibiel, *"A program to analyze the origin of noise in ultra-stable quartz resonators"*, Proc. Joint Meeting IEEE Ann. Freq. Cont. Symp. and European Frequency and Time Forum, Genova, Switzerland, 29 May-1 June, pp. 1176-1181, (2007).

[3] F. Sthal, S. Galliou, X. Vacheret, R. Brendel, P. Salzenstein, E. Rubiola, G. Cibiel *"Analysis of noise origin in ultra stable resonators: preliminary results"*, Proc. 20th European Frequency and Time Forum, Toulouse, France, 25-27 April, FPE-0057.pdf, (2008).

[4] F. Sthal, S. Galliou, J. Imbaud, X. Vacheret, P. Salzenstein, E. Rubiola , G. Cibiel, *"The effect of power-drive level on the calibration of the bridge instrument for the measurement of the quartz stability",* Proc. Joint Meeting IEEE Ann. Freq. Cont. Symp. and European Frequency and Time Forum, Besançon, France, 20-24 April, pp. 487-491, (2009).

[5] A. Ballato, J.G. Gualtieri, *"Advances in High-Q piezoelectric resonator materials and devices",* IEEE Trans. Ultrason. Ferroelec. Freq. Contr., vol. 41, pp. 834-844, (1994).

[6] D.S. Stevens, H.F. Tiersten, *"An analysis of doubly rotated quartz resonators utilizing essentially thickness modes with transverse varation"*, J.A.S.A., Vol. 79, No. 6, pp. 1811-1826, June 1986.

[7] J.J Boy, B. Boizot, R. Petit, D. Picchedda, J.P. Romand, *"Acoustic losses in quartz and their links with InfraRed measurements"*, Proc. Joint Meeting IEEE Ann. Freq. Cont. Symp. and European Frequency and Time Forum, Genova, Switzerland, 29 May-1 June, pp. 199-202, (2007).

[8] B. Sawyer, *"International Round Robin in Infrared Alpha on Measurements on Slices of Synthetic Quartz",* IEEE Trans. Ultrason. Ferroelec. Freq. Contr., vol. 41, pp. 467-472, (1994).